

Article

Shear Tests on Subassemblies Representing the Single-Anchored Connection between Precast Concrete Wall Panels and Reinforced Concrete Frames

Chanwoo Park ^{1,*} , Sookyoung Ha ², Geuntaeck Song ³, Ho Choi ⁴  and Sungyong Yu ⁵

¹ Department of Technical Engineering, Dongsu PCC, Ltd., Seoul 05836, Republic of Korea

² Department of Building Research, Korea Institute of Civil Engineering and Building Technology, Goyang-Si 10223, Republic of Korea; sookyoungha@kict.re.kr

³ Department of Technical Engineering, Hilti (Korea) Ltd., Seoul 05836, Republic of Korea; geuntaeck.song@hilti.com

⁴ Department of Architecture, Shizuoka Institute of Science and Technology, Toyosawa 2200-2, Fukuroi 437-0032, Japan; choi.ho@sist.ac.jp

⁵ Department of Architecture Engineering, Dongguk University, Seoul 04620, Republic of Korea; ysy@dongguk.edu

* Correspondence: dustmqanswp@naver.com

Abstract: Many deformations occur in old RC structures, and the method of reinforcing them using PC members standardized and manufactured in the same mold has difficulty in coping with all deformations (construction error); as a solution to this, overlapping anchor shear connections consisting of three concrete segments have been proposed. This study proposes a special connection for strengthening existing reinforced concrete (RC) framed structures that are more than 30 years old with precast concrete (PC) members. The proposed overlapped anchor connection consists of two anchor groups installed in three concrete segments, which can accommodate deformation by adjusting the height of the concrete connection segment. In this study, the unique shear behavior of the overlapped anchor connection was investigated by analyzing the shear resistance of the single-anchor connection with one post-installed anchor and one cast-in anchor. Eleven specimens of anchored connection models were constructed and push-out tested, and the experimental parameters were analyzed. The shear strength of the single-anchor connection was calculated using a proposed design formula based on the American anchor design code, and the shear strength ratios of the experimental shear strengths to the calculated values were 0.93 on average. The proposed design formula can predict the shear behavior and expected effects of the proposed connection even in differing designs.

Keywords: precast concrete; shear; single anchor; cross-anchor connection; push-out test



Citation: Park, C.; Ha, S.; Song, G.; Choi, H.; Yu, S. Shear Tests on Subassemblies Representing the Single-Anchored Connection between Precast Concrete Wall Panels and Reinforced Concrete Frames. *Buildings* **2023**, *13*, 2632. <https://doi.org/10.3390/buildings13102632>

Academic Editor: Rajai Zuheir Al-Rousan

Received: 22 September 2023

Revised: 17 October 2023

Accepted: 18 October 2023

Published: 18 October 2023



Copyright: © 2023 by the authors. Licensee MDPI, Basel, Switzerland. This article is an open access article distributed under the terms and conditions of the Creative Commons Attribution (CC BY) license (<https://creativecommons.org/licenses/by/4.0/>).

1. Introduction

Driven by recent earthquakes of magnitude five or higher that have occurred in Korea, the seismic retrofitting of old buildings is actively ongoing. Most of the buildings subjected to seismic retrofitting are low-rise reinforced concrete (RC)-framed buildings with identical external bay sizes, including schools, government offices, and military buildings. In order to conveniently and economically retrofit these structures against lateral forces due to seismic loads, the brick infill walls of the exterior frames of the building can be replaced with rigid precast concrete (PC) walls (Frosch et al. [1], 1996; Kesner and Billington, 2005 [2]; Akin and Sezer, 2016 [3]). However, many deformations can occur in old RC structures, and standardized PC members produced in the same mold have difficulty coping with these deformations (construction errors).

As a solution to this, an overlapping anchor connection can be proposed as a height-adjustable connection (Ha et al., 2018) [4]. This is a shear connection consisting of three concrete segments: the RC element, a cast-in-place connection, and a PC wall panel. Cast-in

anchors are installed in the PC panel, and post-installed anchors are installed in the RC elements. The two anchor groups overlap at the cast-in-place connection. As a result, the overlapping anchor connections can solve deformation issues arising from the aging of existing buildings.

Previous experiments [4] have demonstrated the general shear behavior of multi-anchor connections, but experimental studies on the experimental parameters affecting shear behavior are insufficient. In particular, in order to understand the unique behavior of the overlapping anchors, it is necessary to analyze the experimental behavior of a single-anchor connection by removing the parameters of the anchor group. In this regard, the shear behavior of multi-anchor connections has been tested in a previous study on overlapping anchor connections. The construction process was convenient, and the high shear strength required for strengthening was confirmed through experiments.

Furthermore, a shear design formula for the connection between the three different concrete segments with two anchor groups was proposed based on the American anchor design code (ACI Committee 318, 2014) [5] for a connection between two concrete segments. The tested average shear strength of the overlapping multi-anchor connections was 109% of the calculated values.

The studies by Son et al. (2018) [4], Ha et al. (2015) [6], and Yu et al. (2015) [7] were the first to conduct experimental and analytical studies on the relationship between cast-in anchors and post-installed anchors and three different concrete segments. On the other hand, experimental studies on shear resistance with only one type of anchor can be found in a number of papers [8–15]. Examples of existing domestic studies on the shear behavior only of cast-in anchors include that by Kim and Kim (2003) [16]. This paper reported on the experimental shear behavior of each of the domestic high-load anchors or wedge anchors inserted into concrete. The shear strength, pry-out strength, and concrete breakout strength were measured according to one parameter (edge distances) for plain concrete. Additionally, the experimental results were compared to values calculated using the ACI 318-02 guide [17].

In 2018, Vella et al. [18] conducted a study on the design and behavior of the connections between precast concrete elements using overlapping headed bars. These are connections filled with cast-in concrete and can be used to solve the issue of the tensile and shear forces generated between hollow-core PC slabs and PC rim beams. Based on the experimental results, a nonlinear finite element analysis model was proposed.

Recent experimental studies of a shear resistance joint using push-out test anchors or studs similar to those in this study can be found in many papers. Among the studies similar to this study, many experiments have been conducted on steel stud connections in recent years. These studies have mainly conducted experiments on steel stud connections, comprising push-out tests and programs [19–22].

Meanwhile, research on concrete connections has also been conducted. These studies were analyses using concrete structures and pushing tests carried out on anchored connections and concrete connections, and also included PC panel junctions and programs. As such, many studies are being conducted on the connections of the three concrete segments [23–25]. Therefore, as recent studies show, most studies on concrete connections comprise steel stud experiments and push-out tests of connections using only concrete structures. Studies on concrete connections using overlapping anchor connections are insufficient.

Referring to the analysis of previous studies associated with anchor connections and stud connections, the behavior of anchor connections is influenced by several factors, including the strength of the anchor steel, the number of anchors, the arrangement of the anchors, and the edge distance. In this study, the strength of the anchor steel and number of anchors were excluded as experimental parameters. Instead, the thickness, width, and height of the connection, the embedment depths of anchors, the spacing between anchors, the use of a shear stirrup, and the location of the post-installed anchors were varied in order to understand their impact on shear behavior. Eleven shear connection specimens

were tested by applying an upward load to confirm the failure mode of the connection by pure shear load, without applying compressive stress. The shear strength and failure mode of all specimens were calculated using the shear design formula proposed in a previous study by Son et al., and Chapter 17 of the ACI 318M-14 [1] design guide. The calculated values were then compared with the experimental results.

2. Overlapping Anchored Connections

Overlapping anchored connections can be used as height-adjustable shear connections when RC frames are strengthened by introducing PC panels. These shear connections are installed at the bottom of the RC beam and the top of the vertical part of the PC panels, at the location where the largest shear force and displacement are expected under lateral earthquake loading. To resist these forces, multiple chemical anchors ($\phi 24$) are installed, with post-installed anchors at the bottom of the RC beam and cast-in anchors at the top of the PC wall panel arranged to intersect with each other. Additionally, deformed bars are used as stirrups at the top shear connection and high-strength mortar with good flowability is used for finishing. In this study, one cast-in anchor and one post-installed anchor were installed for each specimen to conduct an experimental investigation on the single-anchor connection.

3. Experimental Materials and Method

3.1. Specimens

In total, eleven shear connection specimens were designed and tested in this study. Figures 1 and 2 present the dimensions and reinforcement details of a typical specimen of PCST. Two RC elements were positioned on top of the foundation, and the PC members were placed between them, as shown in Figure 1. The dimensions and reinforcement details of the RC element were consistent across all specimens, with a section size of 450×330 mm. The longitudinal bars consisted of eight deformed bars with a diameter of 16 mm, while the stirrups were deformed bars with a diameter of 10 mm, spaced 150 mm from the end. The PC panel section had dimensions of 700×460 mm, with a thickness matching that of the connection. The longitudinal bars for the PC panel were eight deformed bars with a diameter of 16 mm, and stirrups with a diameter of 10 mm, spaced 50 mm from the end. A cast-in-place anchor was installed on the PC member, and a post-installed anchor was installed on the RC element.

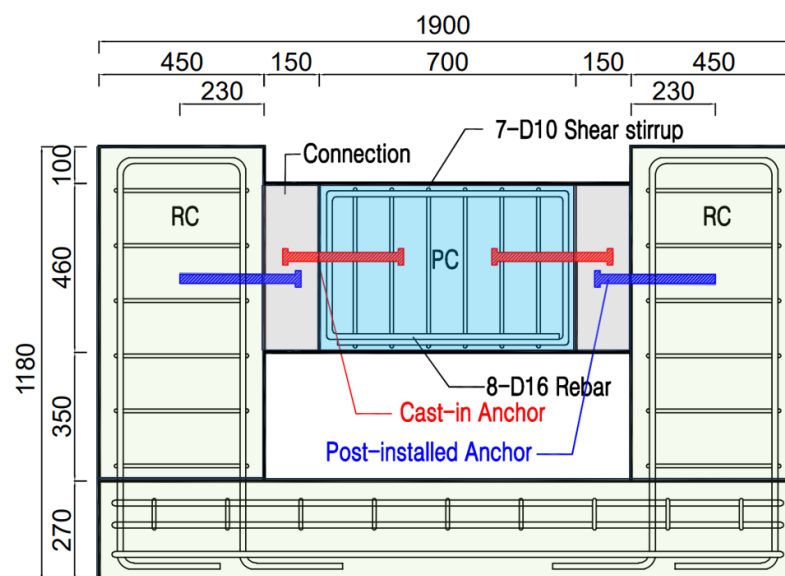


Figure 1. Representative model of the longitudinal section of the PCST specimen.

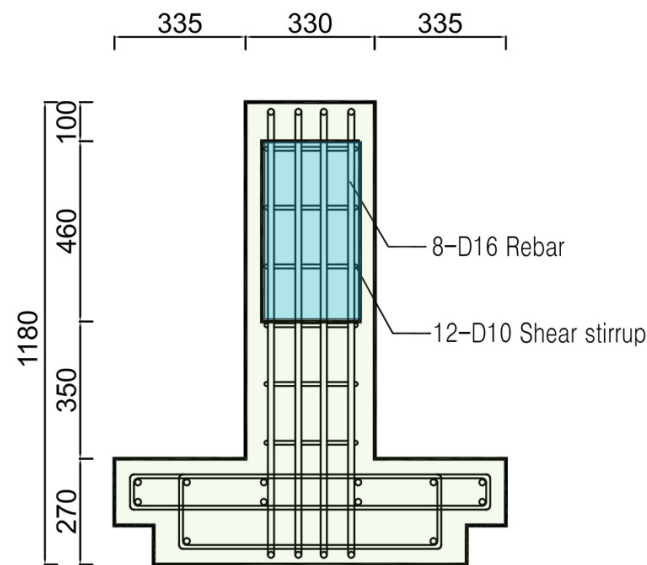


Figure 2. Representative model of the cross-section of the PCST specimen.

3.2. Materials

The compressive strength of the concrete for each specimen at the time of the tests is presented in Table 1. The tensile strengths of the rebars utilized in the specimens are listed in Table 2. Post-installed anchors in the RC member were fixed using chemical anchors ($\phi 24 \times 330$ or 355 mm) supplied by the European company Hilti, Seoul, Republic of Korea, (HY-200 + HIT-V M24). Cast-in anchors installed in the PC wall panel were fixed using welded stud anchors ($\phi 24 \times 330$ or 355 mm). The properties of the anchors utilized in all specimens are summarized in Table 3.

Table 1. Compressive strength of the concrete component.

Specimen	PC Wall Panel (MPa)	RC Frame (MPa)	Connection Strength (MPa)
PCST	23.8	17.9	51.8
PCS25	26.8	23.3	52.0
PCW170	26.8	23.3	52.0
PCW330	26.8	23.3	52.0
PCT100	19.6	27.3	44.4
PCH360	19.6	27.3	44.4
PCH560	19.6	27.3	44.4
PCS100	26.2	18.4	60.2
PCBD10	26.2	18.4	60.2
PCBD16	23.3	18.9	50.3
PCR	23.3	18.9	50.3
Average strength	23.8	22.2	51.1

Table 2. Properties of the reinforcing bars.

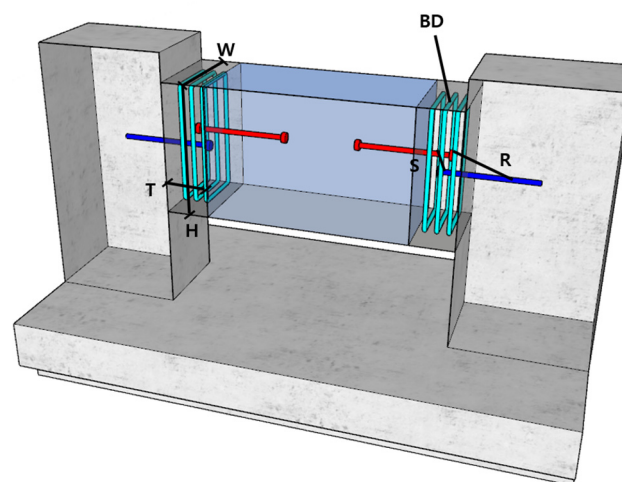
Rebar	Diameter (mm)	Installation Location	Yield Strength (MPa)	Tensile Strength (MPa)
D10	9.5	Shear reinforcing bar of PC and RC members	525.9	645.8
D16	15.9	Main bar of the PC and RC members; horizontal bar of the RC member foundation	575.1	654.4

Table 3. Anchor properties.

Anchor	Installation	Effective Cross-Sectional Area (mm ²)	Yield Strength (MPa)	Tensile Strength (MPa)
Stud	Cast-in-place	353	350	450
Chemical	Post-installed	353	400	500

3.3. Test Parameters

The compressive shear strengths of the overlapped anchored connections were investigated by varying several parameters, including the height, thickness, and width of the connection, anchor spacing, shear stirrups, and the location of the post-installed anchors. The locations of each parameter for the specimens are illustrated in Figure 3, and the details and characteristics of each parameter of the shear connection for all specimens are presented in Table 4.

**Figure 3.** Location of each specimen variable.**Table 4.** Variables of the Shear Connection Specimens.

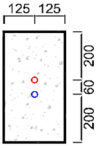
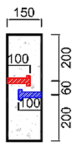
Specimen	Longitudinal Section of the Connection	Cross-Section of the Connection	Anchor Spacing (mm)	Connection Height (mm)	Connection Width (mm)	Connection Thickness (mm)	Shear Stirrup	PC Anchor Depth (mm)	RC Anchor Depth (mm)
PCST			60	460	250	150	-	230	230

Table 4. Cont.

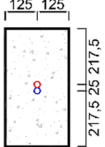
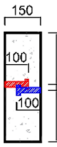
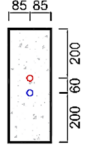
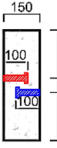
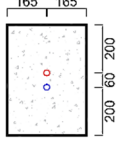
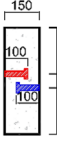
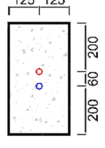

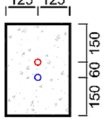
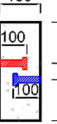
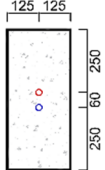
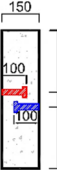
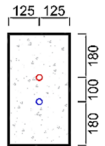
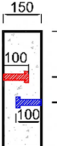
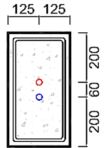
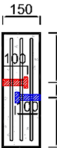
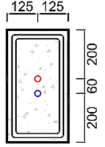
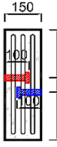
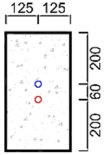
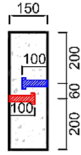
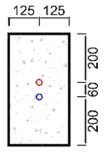
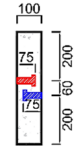
Specimen	Longitudinal Section of the Connection	Cross-Section of the Connection	Anchor Spacing (mm)	Connection Height (mm)	Connection Width (mm)	Connection Thickness (mm)	Shear Stirrup	PC Anchor Depth (mm)	RC Anchor Depth (mm)
PCS25			25	460	250	150	-	230	230
PCW170			60	460	170	150	-	230	230
PCW330			60	460	330	150	-	230	230
PCT100			60	460	250	100	-	255	255
PCH360			60	360	250	150	-	230	230
PCH560			60	560	250	150	-	230	230
PCS100			100	460	250	150	-	230	230
PCBD10			60	460	250	150	D10	230	230
PCBD16			60	460	250	150	D16	230	230

Table 4. Cont.

Specimen	Longitudinal Section of the Connection	Cross-Section of the Connection	Anchor Spacing (mm)	Connection Height (mm)	Connection Width (mm)	Connection Thickness (mm)	Shear Stirrup	PC Anchor Depth (mm)	RC Anchor Depth (mm)
PCR			60	460	250	150	-	230	230
PCT100			60	460	250	100	-	255	255

Note: Compared with the standard PCST test specimen the PCR specimen is a variable in which the cast-in-place anchor and the post-installed anchor are installed in reverse on-site.

(1) Connection height (H)

In the standard PCST test specimen, the height of the connection was 460 mm. For specimens PCH360 and PCH560, the height was reduced to 360 mm and increased to 560 mm, respectively.

(2) Connection thickness (T)

The thickness of the connection for the standard PCST test specimen was 150 mm. For the comparative PCT 100 specimen, the thickness was reduced to 100 mm.

(3) Connection width (W)

In the standard PCST test specimen, the width of the connection was 250 mm. For specimens PCW170 and PCW330, the width was reduced to 170 mm and increased to 330 mm, respectively.

(4) Anchor spacing (S)

The distance between the cast-in-place and post-installed anchors at the connection of the standard PCST test specimen was 60 mm. For specimens PCS25 and PCS100, the spacing between the anchors was reduced to 25 mm and increased to 100 mm, respectively.

(5) Use of stirrups (BD)

The standard PCST test specimen did not have a shear reinforcing bar at the connection. SD400 D10 and SD400 D16 rebars were installed as shear reinforcing bars for specimens PCBD10 and PCBD16, respectively.

(6) Anchor installation location (R)

The connection of the standard PCST test specimen consisted of a cross-anchor connection made by locating a cast-in-place anchor installed on the PC wall panel at the top and a post-installed anchor installed in the RC frame at the bottom. The PCR specimen was a variable in which the cast-in-place and post-installed anchors were installed in reverse.

The embedment depths of the post-installed anchors were 230 mm for the RC and 100 mm for the connection elements. The embedment depth of the cast-in anchors was 230 mm for the PC wall panel and 100 mm for the connection.

3.4. Experimental Method

The foundation of each specimen was installed on a rigid floor using eight steel bars, each with a diameter of 36 mm. An upward load was applied to the bottom center of the PC member using an actuator. Through this method, the pure shear behavior in the

shear connection could be evaluated by inhibiting the compressive force generated by the moment.

The actuator was fixed to a rigid wall using two steel blocks (A and B) and multiple bolts. Steel block A was installed on the rigid wall using 12 steel bars, each with a tensile strength of over 50 tons, as shown in Figures 4 and 5. The actuator was installed on steel block B. Steel blocks B and A were connected to an air impact wrench using more than 100 M24 bolts. The frontal view of the test specimen is depicted in Figure 6.

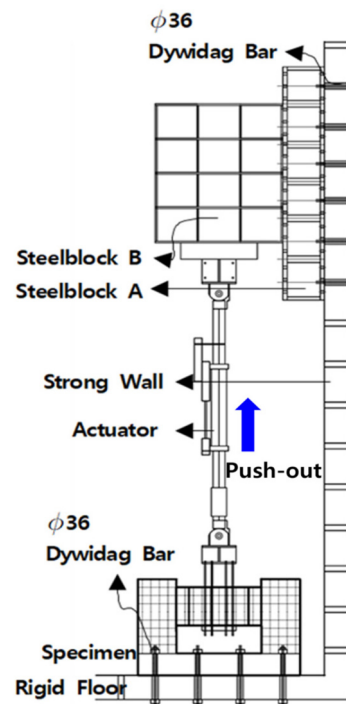


Figure 4. Installation diagram of the test specimen.



Figure 5. Steel block.

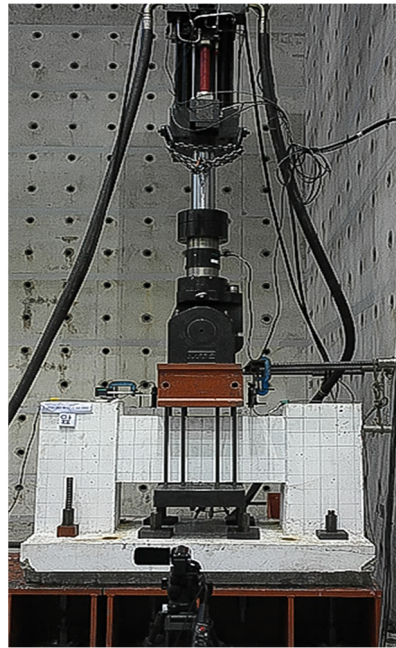


Figure 6. Frontal view of the test specimen.

Displacement-controlled tests were conducted at a loading speed of 0.25 mm/s. When complete shear failure occurred, the specimen was deemed to have been destroyed, and the loading was stopped. Load–displacement curves were plotted, and the failure mechanism was observed and recorded during the test. All cracks in the specimens were marked after testing.

An eccentric load was not applied to either connection to allow for a pure shear failure. To confirm that no eccentric loading occurred, the eccentricity was examined using two linear variable differential transformers (LVDTs Seoul, Republic of Korea). The LVDTs were installed on top of the PC members at 600 mm intervals. According to the measurements, eccentricity did not occur because the displacement at the maximum load differed by approximately 0.05 mm on average. In addition, no slipping occurred in any of the specimens, and no lateral displacements were observed.

4. Experimental Results and Variable Analysis

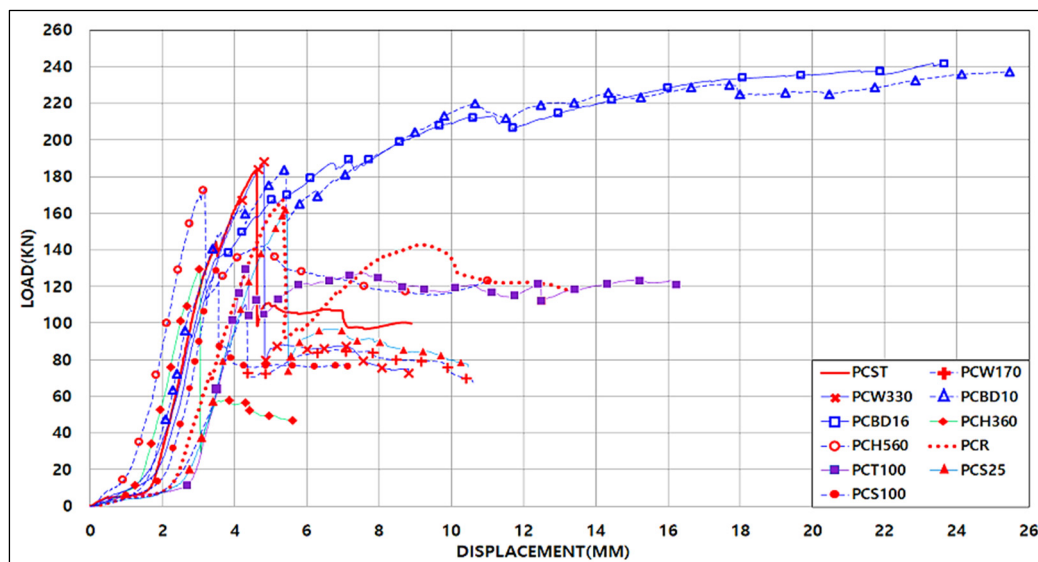
4.1. Experimental Method

The experiment and calculation results for the maximum load, displacement at the maximum load, and final failure site (section, RC column, and PC member) are presented in Table 5. Load–displacement curves for all the test specimens are shown in Figure 7. During the experiment, the maximum load at the center of the PC member was distributed between both connections, confirming that the shear strength of one connection was half of the maximum load. The standard test specimen (PCST) had a shear strength of 91.8 kN and a displacement of 4.6 mm at the maximum load. The specimen with the largest shear strength was PCBD16, which had a 3-D16 shear reinforcing bar at the connection, with a strength of 120.9 kN and a displacement of 23.7 mm at the maximum load.

Table 5. Component experimental results—maximum load, displacement, and failure mode.

Specimen	Maximum Load (kN)	Shear Strength (kN)	Ratio	Displacement at Maximum Load (mm)	Failure Mode
PCST	183.5	91.8	1.00	4.6	Breakout at Connection
PCS25	162.3	81.2	0.88	5.5	Breakout at Connection
PCW170	110.9	55.5	0.60	4.3	Breakout at Connection
PCW330	188.2	94.1	1.03	4.8	Breakout at Connection
PCT100	130.6	65.3	0.71	4.4	Breakout at Connection
PCH360	129.6	64.8	0.71	3.1	Breakout at Connection
PCH560	173.3	86.7	0.94	3.2	Breakout at Connection
PCS100	129.1	64.6	0.70	3.5	Breakout at Connection
PCBD10	237.3	118.7	1.29	25.5	Breakout at PC
PCBD16	241.8	120.9	1.32	23.7	Breakout at PC
PCR	167.3	83.7	0.91	5.4	Breakout at Connection

Note: The ratio is based on the shear strength of the standard PCST test specimen.

**Figure 7.** Experimental results—comparison of load–displacement curves.

A comparison of load–displacement curves for all test specimens by variable compared to the subject PCST is shown in Figure 8. In more detail than Figure 7, the load and displacement were shown when compared with the PCST experiment for each variable.

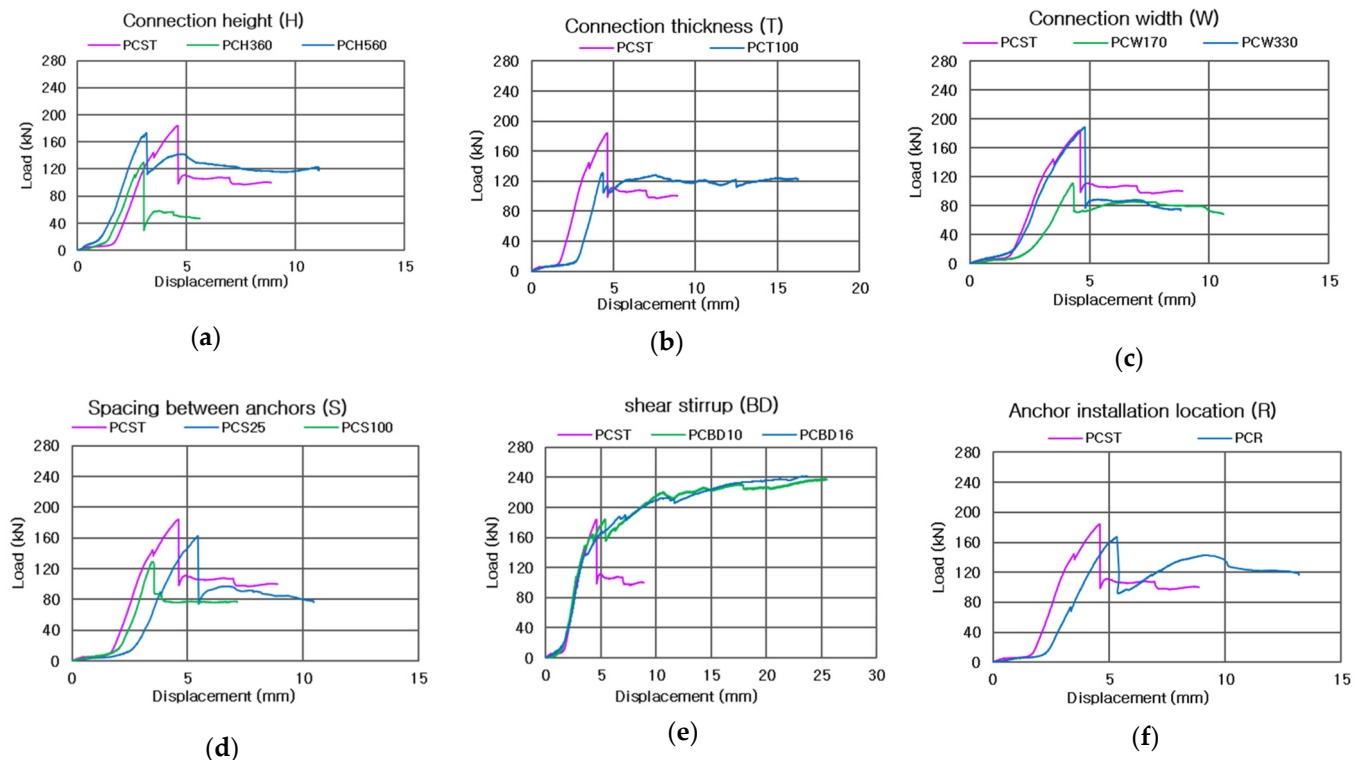


Figure 8. Comparison of PCST specimens and load–displacement curves by variable: (a) connection height (H); (b) connection thickness (T); (c) connection width (W); (d) anchor spacing (S); (e) using a stirrup (BD); (f) anchor installation location (R).

The crack patterns shown in Figure 9 indicate that the specimens failed due to breakout failure. Figure 10 shows an image of the crack in the standard test specimen (PCST) after the experiment. At its maximum strength of 183.5 kN, a diagonal crack developed 100 mm downward to the upper-right part of the connection, and the strength decreased sharply. In PCBD10 and PCBD16, which had shear reinforcing bars installed, no cracks were observed at the connection. However, vertical cracks developed between the PC member and the connection, and a diagonal field crack led to specimen failure (Figures 11 and 12). Therefore, only the PC members of specimens with shear reinforcing bars installed at their connections failed.

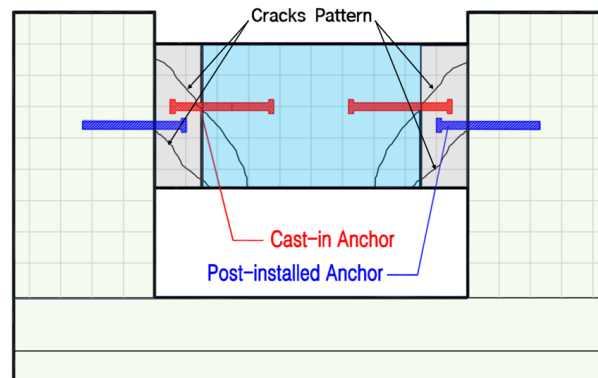


Figure 9. Initial cracks developed at the connection of the RC member and advanced into breakout failure.

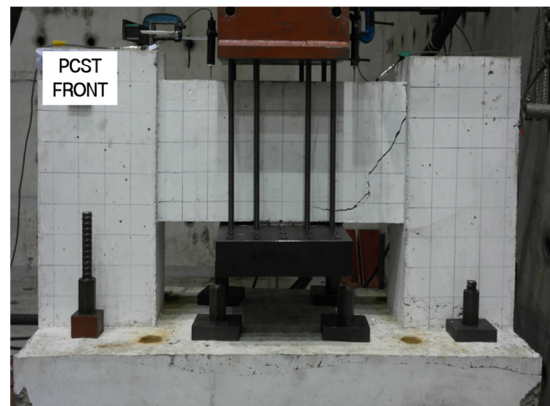


Figure 10. Cracks in the PCST specimen.

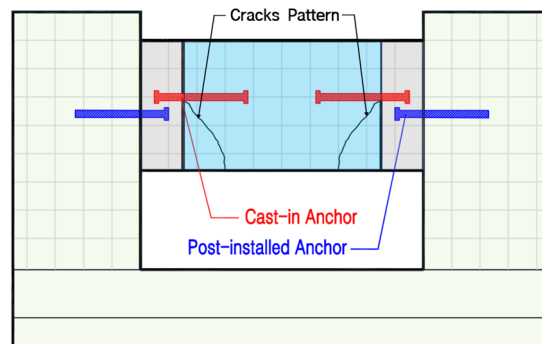


Figure 11. Initial cracks developed at the connection of the PC member and advanced into breakout failure.

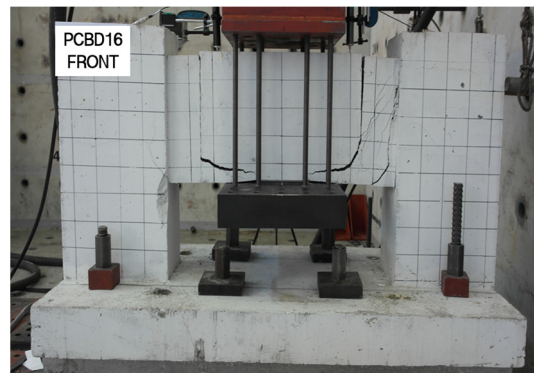


Figure 12. Cracks in specimen PCBD16.

4.2. Comparison of Experimental Variables

(1) Connection height (H)

The shear strength of specimen PCH560 with a connection height of 560 mm and the standard specimen (PCST) with a connection height of 460 mm differed by approximately 6%. However, when the connection height was lowered to 360 mm, as in the case of specimen PCH360, the shear strength was reduced by approximately 29% compared with that of the standard specimen. This reduction occurred because when the connection height is decreased, the edge distance of the concrete vertical to the force direction also decreases. This decrease resulted in a smaller projection area of concrete compared with the standard test specimen, and the range of the projection area was calculated to be smaller than the height of the connection. Similarly, even by increasing the height of the connection in test

specimen PCH560, the projection area due to breakout failure would be the same as that of the standard test specimen; thus, the two specimens should exhibit similar shear strengths.

(2) Connection thickness (T)

The shear strength of specimen PCT100, which had a reduced connection thickness of 100 mm, decreased by approximately 29% compared with the standard test specimen (PCST), which had a connection thickness of 150 mm. As the connection thickness decreased, it was installed as 75 mm, which is smaller than the effective insertion depth $h_{ef} = \max [(125/1.5), (60/3)] = 83.3$ mm required by the ACI 318-14 [5]; thus, the connection exhibited reduced shear behavior, resulting in a lower strength.

(3) Connection width (W)

Compared with the standard PCST test specimen, which had a connection width of 250 mm, the shear strength of specimen PCW170, which had a connection width of 170 mm (0.68 times that of the standard test specimen), decreased by 40%. Moreover, the shear strength slightly increased by 3% in specimen PCW330, which had a width of 330 mm (1.32 times that of the standard test specimen). Thus, a reduction in the connection width has a considerable effect on the shear strength. In a similar manner to variations in the connection height, the shear strength value decreased as the projection area decreased due to the decrease in the connection width.

(4) Spacing between anchors (S)

Compared with the standard PCST test specimen, which had a spacing of 60 mm between the cast-in-place and post-installed anchors, the shear strengths of specimens PCS25 and PCS100, with spacings of 25 mm and 100 mm between the anchors, decreased by 12% and 30%, respectively. As the spacing between the anchors narrowed, specimen PCS25 was affected by interference between the anchors, whereas test specimen PCS100 encountered failure at a lower strength than the standard test specimen due to the reduced concrete edge distance.

(5) Using shear stirrup (BD)

Adding shear reinforcing bars at the connection improved both the shear strength and ductility of the connection. The shear strengths of specimens PCBD10 and PCBD16 increased by 29% and 32%, respectively, compared with the standard PCST test specimen without shear reinforcing bars. In addition, the specimens with shear reinforcing bars exhibited ductile behavior, as observed in the load–displacement curve in Figure 7. The failure mode of the standard test specimen was breakout failure, which generated 100 mm diagonal cracks downward on the upper-right corner of the connection. In contrast, specimens PCBD10 and PCBD16 did not crack at the connection but developed vertical cracks between the PC member and the connection, which then led to diagonal cracks and fractures. Fracture only occurred on the PC members of specimens that had shear reinforcing bars installed at the connection. These results confirm that the shear strength and ductility of the connection can be effectively increased by augmenting the connections with shear reinforcing bars.

(6) Anchor installation location (R)

The standard test PCST specimen was installed above the cast-in-place anchor, close to the loading unit, whereas specimen PCR was installed on the upper side of the post-installed anchor. The shear strength of specimen PCR decreased by 9% compared with that of the standard test specimen. This was likely due to the edge distance (spacing between anchors) of the concrete failure site being reduced by 60 mm compared with that of specimen PCST.

Based on a comparative analysis of the experimental results from all the specimens using the above variables, it was confirmed that as the dimensions of related elements, such as the connection, base material, and anchor insertion depth, are reduced, the shear

strength value decreases because the projection area affecting the shear strength of concrete also decreases.

5. Comparison with Calculation Results

5.1. Analysis Method

In the study, the nominal shear strength of the anchor used in the specimens was analyzed based on the standard anchor shear strength stipulated in Chapter 17 of ACI 318M-14 [5]. The anchor steel strength and breakout strength of the PC member, RC member, and connection were separately analyzed (Appendix A). The experimental results showed that pry-out failure did not occur because the concrete limited the displacement of the anchor. Therefore, the minimum breakout failure strength, which was the same as the failure mode observed in the experiment, was calculated as the shear strength of the connection and compared with the experimental results.

The equation for the nominal concrete failure strength for the single anchor connection, which was determined through the experiment, was assumed to have a variation rate of 15% and a 5% quartile value. This value was used to compare the calculation and experimental results. To maintain consistency with the experimental conditions, the value was set to be the same in the calculation as in the experiment. In Equation (1), $F_{5\%}$ represents the characteristic strength (5% quartile), while in Equation (2), F_m represents the average strength.

$$F_{5\%} = F_m(1 - K_v) \quad (1)$$

$$F_m = (1 / (1 - 1.645 \times 0.15)) F_{5\%} = 1.33 F_{5\%} \quad (2)$$

Based on ACI 355 (2011) [3], the value of K was used to calculate the characteristic strength in the 90% reliability range. In the case of an infinite number of experiments, K is set to 1.645. If the variation rate is 15%, v , the variation rate, is set to 0.15. Therefore, the nominal concrete failure strength coefficient of the anchor (1.33) was multiplied and reflected in the shear strength calculation, as shown in Equation (2). Additionally, the number of anchors and the projection area of the anchor were adjusted according to the shear strength calculation formula for the cross-anchor connection proposed in the previous multi-anchor study to predict the shear strength of the single cross-anchor connection.

5.2. Comparative Analysis Method between the Calculation and Experimental Results

The experiment and analysis results were compared for shear strength, and the comparison graphs are shown in Figure 13; the summarized results in Table 6 compare the main failure locations observed in the experiment with the failure locations predicted in the calculation. In most cases, the shear strength measured in the experiment was either similar to or lower than that in the calculation results. This is because variables that could not be reflected in the calculation affected the experimental results.

For specimens PCBD10 and PCBD16, which had shear reinforcing bars, the experimental results were predicted to be approximately 5% to 8% different from the calculation results. The joint was calculated by applying the coefficient, considering that it could receive a reinforcing effect similar to that of $\psi_{c,V}$, which is the criterion for the modification coefficient of the shear reinforcing bar in ACI 318M-14 17.5.2.7. [5] Furthermore, both test specimens that had shear reinforcing bars were interpreted to have experienced breakout failure in their PC members, which was consistent with the experimental results.

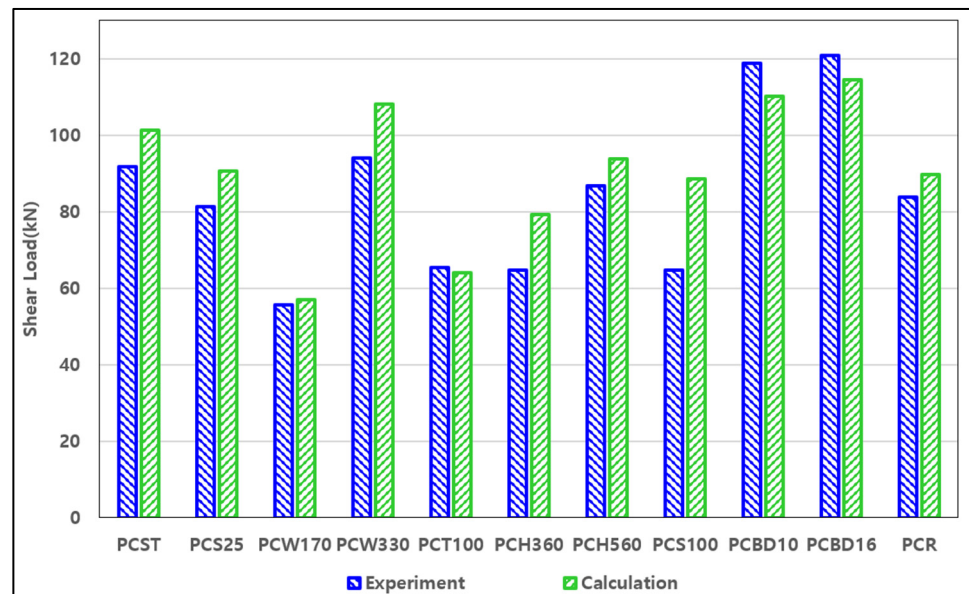


Figure 13. Comparison between shear strengths obtained from the experiment and calculation.

Table 6. Comparison of the calculated and experimental shear strengths.

Test Specimens	Shear Strength (kN)			Failure Location	
	Experiment	Calculation	Ratio (%)	Experiment	Calculation
PCST	91.8	101.3	0.91	Breakout at Connection	
PCS25	81.2	90.5	0.90	Breakout at Connection	Breakout at PC
PCW170	55.5	56.9	0.98	Breakout at Connection	
PCW330	94.1	108.1	0.87	Breakout at Connection	
PCT100	65.3	63.9	1.02	Breakout at Connection	
PCH360	64.8	79.3	0.82	Breakout at Connection	
PCH560	86.7	93.8	0.95	Breakout at Connection	
PCS100	64.6	88.5	0.73	Breakout at Connection	Breakout at PC
PCBD10	118.7	110.1	1.08	Breakout at Connection	
PCBD16	120.9	114.5	1.05	Breakout at Connection	
PCR	83.7	89.8	0.93	Breakout at Connection	

Note: The experimental shear strength is half the shear strength at the maximum load shown in the ratio, which is between the experimental shear strength and the calculated shear strength.

In specimens PCBD10 and PCBD16, three strands of D10 and D16 shear reinforcing bars were installed at intervals of 40 mm. However, the modification coefficient of the shear reinforcing bar $\psi_{c,V}$ from ACI 318M-14 17.5.2.7 [5] uses an auxiliary bar and should be multiplied by the $\psi_{c,V} = 1.4$ coefficient when using a D13 reinforcing bar at intervals of less than 100 mm. Although an auxiliary reinforcing bar was not installed in the specimens used in this study, the interval set was more than 50 mm narrower than the standard, and a D16 shear reinforcing bar was used; hence, it was estimated that a similar reinforcing effect could be generated, and a coefficient of 1.4 was applied. As a result, the shear strength of the PC member was predicted to be lower than the shear strength of the connection, which coincided with the experimental results for the actual PC member, and similarly, the strength increased. To this end, the experiments and analyses cross-validated that the shear strength of the connection increased when a shear reinforcing bar was used.

After calculating the strength of each part of the cast-in-place and post-installed anchors, the shear strength was calculated at the minimum breakout strength. Hence, the spacing between the anchors was not considered in the calculation formula. Therefore, there was a difference in the failure location between the experiments and calculation for specimens PCS25 and PCS100, and in specimen PCS100, which had a relatively large spacing between the anchors; there was approximately a 27% difference between the experimental and calculation results.

Except for specimens PCS25 and PCS100, both the calculation and experimental results predicted that failure would occur at the same location. Therefore, it was confirmed that the failure location of a single cross-anchor connection could be calculated using the ACI 318-14 [5] calculation formula. Specimens PCS25 and PCS100 were considered to be errors and experimental variables due to changes in the distance between anchors that were not considered in the calculation method. Thus, further research on the distance between anchors is needed to improve the reliability of the calculation method. Further research is needed, with examples of future studies including adding a coefficient that considers the effect of the distance between anchors.

6. Conclusions

In this study, 11 shear model test specimens using cast-in-place and post-installation anchors, which provided a vertical connection between the RC and PC members with three different layers of concrete, were tested, and the results were compared with the ACI 318M-14 calculation formula. The experiment confirmed the anchor's unique behavior according to each variable and connection, and yielded the following conclusions:

- (1) Depending on the push-out experimental loading, initial cracks occurred in between RC and PC members and connections. Two dangerous cross-sections were observed in the anchor connection, this crack propagated into diagonal shear cracks at the anchor connection. The final failure location was consistent in nine specimens excluding two PCS specimens, and the error rate of shear strength was approximately 7% or less. Therefore, this study concludes that the ACI 318M-14 calculation formula is reliable for design purposes.
- (2) The experimental results of specimens PCS25 and PCS100, where the vertical spacing between the two anchors was varied, showed a strength difference of up to 27% compared with the calculation results, and the predicted final failure location was also different. The ACI 318M-14 calculation formula is limited to analyzing a single anchor, which is expected to be difficult to apply to the spacing interpretation between the two anchors.
- (3) Future research and experiments related to this study suggest that reliability should be improved by focusing the effects of anchor spacing and shear stirrups as critical variables and adjusting the calculation formula. Furthermore, if additional variables such as anchor insertion depth and use of steel plate connections are verified and compared in future studies, the method presented in this study is expected to be reliable and effective for actual connections with more diverse variables and to increase the reliability of the calculation formula.

Author Contributions: Conceptualization, S.Y.; validation, H.C.; formal analysis, C.P.; investigation, C.P.; resources, S.Y.; writing—original draft preparation, C.P.; writing—review and editing, S.H., G.S. and H.C.; visualization, C.P.; supervision, S.Y.; project administration, S.Y.; funding acquisition, S.H. and S.Y. All authors have read and agreed to the published version of the manuscript.

Funding: This study received support from the Korean government's Ministry of Land, Infrastructure, and Transport through a grant (16CTAP-C077924-03) for the Technology Advancement Research Program (TARP). The researchers also acknowledge Hilti (Korea) Ltd. for their cooperation in the research on shear anchor design.

Data Availability Statement: The data are available upon request from the corresponding authors.

Conflicts of Interest: The authors declare no conflict of interest.

Appendix A

The shear strength of the standard test specimen PCST was analyzed based on the anchor design criteria in Chapter 17 of ACI 318M-14 [5].

(1) Shear strength of the PC cast-in-place anchor

This is a single anchor; therefore, $n = 1$, the cross-sectional area of the anchor $A_{se,V} = 353 \text{ mm}^2$, and the tensile strength $f_{uta} = 500 \text{ MPa}$, $V_{sa} = 1.33(nA_{se,V} f_{uta}) = 234.7 \text{ kN}$.

(2) PC cast-in-place breakout strength

$$V_{cb} = 1.33[(A_{vc}/A_{vco})\psi_{ed,V}\psi_{c,V}\psi_{h,V}V_b] = 51.6 \text{ kN}$$

Because the direction of the minimum edge distance was perpendicular to the direction of the shear force, the doubled value $2V_{cbo} = 103.2 \text{ kN}$ was applied.

$c_{a1} = 125/1.5 = 83 \text{ mm}$, $c_{a2} = 125 \text{ mm}$, $c_{a3} = 125 \text{ mm}$, $h_a = 150 \text{ mm}$, $\lambda_a = 1$, $l_e = 210 \text{ mm}$, $d_a = 25 \text{ mm}$, $\psi_{c,V} = 1.4$, $f_{ck} = 23.8 \text{ MPa}$,

$$A_{Vc} = h_a(c_{a2} + c_{a3}) = 150(125 + 125) = 37,500 \text{ mm}^2$$

$$A_{Vco} = 4.5(c_{a1})^2 = 4.5(83)^2 = 31,000 \text{ mm}^2, \psi_{ed,V} = 0.7 + 0.3c_{a2}/c_{a1} = 1.02 > 1 \therefore \psi_{ed,V} = 1$$

$$\psi_{h,V} = \sqrt{(1.5c_{a1}/h_a)} = 0.73$$

$$V_b = 0.66(l_e/d_a)^{0.2}\sqrt{d_a}\sqrt{f_{ck}}(c_a)^{1.5}/1000 = 30.3 \text{ kN}$$

(3) PC cast-in-place pryout strength The pryout strength was calculated as the sum of the strengths of the PC and connection parts.

a. Pryout strength of the PC part:

$$V_{cp-P} = 1.33\left[k_{cp}\left(\frac{A_{Nc}}{A_{Nco}}\right)\psi_{ed,N}\psi_{c,N}\psi_{cp,N}N_b\right] = 160.4 \text{ kN}$$

where $f_{ck} = 23.8 \text{ MPa}$, $h_{ef} = 210 \text{ mm}$, $k_{cp} = 2.0$, $C_{ac} = 420 \text{ mm}$, $\psi_{c,N} = 1.25$, $k_c = 10$

$$A_{Nc} = (250)(2 \times 1.5 \times h_{ef}) = 157,500 \text{ mm}^2$$

$$A_{Nco} = 9(h_{ef})^2 = 396,900 \text{ mm}^2, \psi_{ed,N} = 0.7 + 0.3\left(\frac{c_{a,min}}{1.5h_{ef}}\right) = 0.82$$

$$\psi_{cp,N} = C_{a,min}/C_{ac} = 0.3$$

$$N_b = k_c\sqrt{f_{ck}}h_{ef}^{1.5} = 148.5 \text{ kN}$$

b. Pryout strength of the RC part:

$$V_{cp-C} = 1.33\left[k_{cp}\left(\frac{A_{Nc}}{A_{Nco}}\right)\psi_{ed,N}\psi_{c,N}\psi_{cp,N}N_b\right] = 215.5 \text{ kN}$$

$f_{ck} = 51.8 \text{ MPa}$, $h_{ef} = 80 \text{ mm}$, $k_{cp} = 2.0$, $C_{ac} = 160 \text{ mm}$, $\psi_{c,N} = 1.25$, $k_c = 10$

$$A_{Nc} = (2 \times 1.5 \times h_{ef}) = 57,600 \text{ mm}^2$$

$$A_{Nco} = 9(h_{ef})^2 = 57,600 \text{ mm}^2, \psi_{ed,N} = 0.7 + 0.3 \left(\frac{c_{a,min}}{1.5h_{ef}} \right) = 1.1$$

$$\psi_{cp,N} = C_{a,min}/C_{ac} = 1.0$$

$$N_b = k_c \sqrt{f_{ck}} h_{ef}^{1.5} = 148.5 \text{ Kn}$$

When the pryout strength of the PC part is added to that of the connection part:

$$V_{cp-P} + V_{cp-C} = 160.4 + 215.5 = 375.92 \text{ kN}$$

(4) Shear strength of the RC post-installed anchor

This is a single anchor; therefore, $n = 1$, the cross-sectional area of the anchor $A_{se,V} = 353 \text{ mm}^2$, and the tensile strength $f_{uta} = 500 \text{ MPa}$, $V_{sa} = 1.33(nA_{se,V} f_{uta}) = 140.8 \text{ kN}$.

(5) RC post-installed breakout strength

$$V_{cb} = 1.33[(A_{vc}/A_{vco})\psi_{ed,V} \psi_{c,V} \psi_{h,V} V_b] = 55.7 \text{ kN}$$

The direction of the minimum edge distance is perpendicular to the direction of the shear force; therefore, $2V_{cbo} = 98.1 \text{ kN}$ was applied.

$c_{a1} = 165 \text{ mm}$, $c_{a2} = 360 \text{ mm}$, $h_a = 450 \text{ mm}$, $\lambda_a = 1$, $l_e = 230 \text{ mm}$, $d_a = 24 \text{ mm}$, $\psi_{c,V} = 1.2$, $f_{ck} = 17.9 \text{ MPa}$; therefore, these values can be substituted into the following equation:

$$A_{Vc} = 1.5 \times c_{a1} \times (2 \times 1.5 \times c_{a1}) = 122,512.5 \text{ mm}^2$$

$$A_{Vco} = 4.5(c_{a1})^2 = 122,512.5 \text{ mm}^2, \psi_{ed,V} = 0.7 + 0.3c_{a2}/1.5c_{a1} = 1.136 > 1 \therefore \psi_{ed,V} = 1$$

$$\psi_{h,V} = \sqrt{(1.5c_{a1}/h_a)} = 0.74$$

$$V_b = 0.66(l_e/d_a)0.2\sqrt{d_a}\sqrt{f_{ck}}(c_a)^{1.5}/1000 = 41.4 \text{ kN}$$

(6) RC post-installed pryout strength The pryout strength was calculated as the sum of the strengths of the RC and connection parts.

a. Pryout strength of the PC part:

$$V_{cp-R} = 1.33 \left[k_{cp} \left(\frac{A_{Nc}}{A_{Nco}} \right) \psi_{ed,N} \psi_{c,N} \psi_{cp,N} N_b \right] = 55.7 \text{ kN}$$

$$f_{ck} = 17.9 \text{ MPa}, h_{ef} = 230 \text{ mm}, k_{cp} = 2.0, C_{ac} = 460 \text{ mm}, \psi_{c,N} = 1.4, k_c = 7$$

$$A_{Nc} = (330)(2 \times 1.5 \times h_{ef}) = 227,700 \text{ mm}^2$$

$$A_{Nco} = 9(h_{ef})^2 = 476,100 \text{ mm}^2, \psi_{ed,N} = 0.7 + 0.3 \left(\frac{c_{a,min}}{1.5h_{ef}} \right) = 0.84$$

$$\psi_{cp,N} = C_{a,min}/C_{ac} = 0.4$$

$$N_b = k_c \sqrt{f_{ck}} h_{ef}^{1.5} = 103.3 \text{ kN}$$

$$V_{cp-C} = 1.33 \left[k_{cp} \left(\frac{A_{Nc}}{A_{Nco}} \right) \psi_{ed,N} \psi_{c,N} \psi_{cp,N} N_b \right] = 189.5 \text{ kN},$$

where $f_{ck} = 51.8 \text{ MPa}$, $h_{ef} = 100 \text{ mm}$, $k_{cp} = 2.0$, $C_{ac} = 200 \text{ mm}$, $\psi_{c,N} = 1.25$, $k_c = 10$

$$A_{Nc} = (250) (2 \times 1.5 \times h_{ef}) = 75,000 \text{ mm}^2$$

$$A_{Nco} = 9(h_{ef})^2 = 90,000 \text{ mm}^2, \psi_{ed,N} = 0.7 + 0.3 \left(\frac{c_{a,min}}{1.5h_{ef}} \right) = 0.95$$

$$\psi_{cp,N} = 1$$

$$N_b = k_c \sqrt{f_{ck}} h_{ef}^{1.5} = 72.0 \text{ kN}$$

After adding the pryout strength of the PC and connection parts,

$$V_{cp-R} + V_{cp-C} = 55.7 + 189.5 = 245.1 \text{ kN}$$

(7) Connection cast-in-place breakout strength

$$V_{cb} = 1.33[(A_{vc}/A_{vco})\psi_{ed,V} \psi_{c,V} \psi_{h,V} V_b] = 50.6 \text{ kN}$$

The direction of the shear force was perpendicular to the direction of the minimum edge distance; therefore, $2V_{cbo} = 111.4 \text{ kN}$ was applied.

$c_{a1} = 125/1.5 = 83 \text{ mm}$, $c_{a2} = 125 \text{ mm}$, $c_{a3} = 125 \text{ mm}$, $h_a = 150 \text{ mm}$, $\lambda_a = 1$, $l_e = 80 \text{ mm}$, $d_a = 25 \text{ mm}$, $\psi_{c,V} = 1$, $f_{ck} = 51.8 \text{ MPa}$; therefore, these values can be substituted into the following equations:

$$A_{Vc} = 70,312.5 \text{ mm}^2, A_{Vco} = 70,312.5 \text{ mm}^2, \psi_{ed,V} = 0.7 + 0.3c_{a2}/c_{a1} = 1.02 > 1 \therefore \psi_{ed,V} = 1$$

$$\psi_{h,V} = \sqrt{(1.5c_{a1}/h_a)} = 1.12 > 1 \therefore \psi_{h,V} = 1$$

$$V_b = 0.66(l_e/d_a)0.2\sqrt{d_a}\sqrt{f_{ck}}(c_a)^{1.5}/1000 = 38.1 \text{ kN}$$

(8) Connection post-installed breakout strength

$$V_{cb} = 1.33[(A_{vc}/A_{vco})\psi_{ed,V} \psi_{c,V} \psi_{h,V} V_b] = 63.3 \text{ kN}$$

The direction of the shear force was perpendicular to the direction of the minimum edge distance; therefore, $2V_{cbo} = 115.1 \text{ kN}$ was applied.

$c_{a1} = 125 \text{ mm}$, $c_{a2} = 200 \text{ mm}$, $h_a = 150 \text{ mm}$, $\lambda_a = 1$, $l_e = 100 \text{ mm}$, $d_a = 24 \text{ mm}$, $\psi_{c,V} = 1$, $f_{ck} = 51.8 \text{ MPa}$; therefore, these values can be substituted into the following equations:

$$A_{Vc} = 37,500 \text{ mm}^2, A_{Vco} = 31,000 \text{ mm}^2, \psi_{ed,V} = 0.7 + 0.3c_{a2}/c_{a1} = 1.02 > 1 \therefore \psi_{ed,V} = 1$$

$$\psi_{h,V} = \sqrt{(1.5c_{a1}/h_a)} = 1.12 > 1 \therefore \psi_{h,V} = 1$$

$$V_b = 0.66(l_e/d_a)0.2\sqrt{d_a}\sqrt{f_{ck}}(c_a)^{1.5}/1000 = 39.3 \text{ kN}$$

Table A1. Shear strength of specimen PCST.

Part	Failure Mode	Strength [kN]
PC panel	Anchor shear	234.7
	Breakout	103.2
	Pryout	160.4
RC column	Anchor shear	140.8
	Breakout	111.4
	Pryout	55.7
Connection (Cast-in-place anchor)	Breakout	101.3
	Pryout	215.5
Connection (Post-installed anchor)	Breakout	126.6
	Pryout	189.5
Minimum strength	Connection failure	101.3

References

1. Frosch, R.J.; Li, W.; Jirsa, J.O.; Kreger, M.E. Retrofit of non-ductile moment-resisting frames using precast infill wall panels. *Earthq. Spectra* **1996**, *12*, 741–760. [\[CrossRef\]](#)
2. Kesner, K.; Billington, S.L. Investigation of infill panels made from engineered cementitious composites for seismic strengthening and retrofit. *J. Struct. Eng.* **2005**, *131*, 1712–1720. [\[CrossRef\]](#)
3. Akin, A.; Sezer, R. A study on strengthening of reinforced concrete frames using precast concrete panels. *KSCE J. Civ. Eng.* **2016**, *20*, 2439–2446. [\[CrossRef\]](#)
4. Son, G.W.; Ha, S.K.; Song, G.T.; Yu, S.Y. Shear tests on subassemblies representing the multi-anchored connection between PC wall and RC frames. *KSCE J. Civ. Eng.* **2018**, *22*, 5164–5177. [\[CrossRef\]](#)
5. *ACI 318M-14*; ACI Committee 318. Building Code Requirement for Structural Concrete and Commentary. American Concrete Institute: Farmington Hills, MI, USA, 2014.
6. Ha, S.K.; Son, G.W.; Yu, S.Y.; Ju, H.S. Shear behavior of existing reinforced concrete frame structures infilled with U-Type precast wall panel. *J. Korea Inst. For. Struct. Maint. Insp.* **2015**, *19*, 18–28.
7. Yu, S.Y.; Song, G.T.; Ha, S.K.; Song, H.S.; Son, G.W. Modeling test of shear connectors between precast concrete members to infill the gap interface. In Proceedings of the Advanced in Civil, Environmental, and Materials Research (ACEM15), Incheon, Republic of Korea, 25–29 August 2015.
8. Anderson, N.S.; Meinheit, D.F. Pryout capacity of cast-in headed stud anchors. *PCI J.* **2005**, *50*, 90–112. [\[CrossRef\]](#)
9. Hoehler, M.S.; Eligehausen, R. Behavior and testing of anchors in simulated seismic cracks. *ACI Struct. J.* **2008**, *105*, 348.
10. Eligehausen, R.; Cook, R.A.; Appl, J. Behavior and design of adhesive bonded anchors. *ACI Struct. J.* **2006**, *103*, 822.
11. Zhang, Y.G.; Klingner, R.E.; Graves, H.L. Seismic response of multiple-anchor connections to concrete. *J. Struct. Eng.* **2001**, *98*, 811–822.
12. Petersen, D.; Zhao, J. Design of anchor reinforcement for seismic shear loads. *ACI Struct. J.* **2013**, *110*, 53.
13. Takase, Y. Testing and modeling of dowel action for a Post-installed anchor subjected to combined shear force and tensile force. *Eng. Struct.* **2019**, *195*, 551–558. [\[CrossRef\]](#)
14. Jebara, K.; Özbolt, J.; Hofmann, J. Pryout failure capacity of anchorages experimental and numerical investigation. In Proceedings of the 3rd International Symposium on Connections between Steel and Concrete, Stuttgart, Germany, 27–29 September 2017.
15. Prakash, A.; Anandavalli, N.; Madheswaran, C.K.; Lakshmanan, N. Modified push-out tests for determining shear strength and stiffness of hss stud connector-experimental study. *Int. J. Compos. Mater.* **2012**, *2*, 22–31. [\[CrossRef\]](#)
16. Kim, S.; Kim, G. *Evaluation of Single Anchor Shear History of Non-Crack Plain Concrete*; Korean Institute for Structural Inspection: Seoul, Republic of Korea, 2003; Volume 7.
17. ACI Committee 355. *Qualification of Post-Installed Adhesive Anchors in Concrete (ACI 355.4-11) and Commentary*; American Concrete Institute: Farmington Hills, MI, USA, 2011.
18. Vella, J.P.; Vollum, R.L.; Kotecha, R. Headed bar connections between precast concrete elements: Design recommendations and practical applications. *Structures* **2018**, *15*, 162–173. [\[CrossRef\]](#)
19. Liang, Z.; Gong, C.; Liang, W.; Zhang, S.; Li, X. Behavior of Confined Headed Bar Connection for Precast Reinforced Concrete Member Assembly. *Appl. Sci.* **2023**, *13*, 827. [\[CrossRef\]](#)
20. Wang, W.; Zhang, X.D.; Zhou, X.L.; Zhang, B.; Chen, J.; Li, C.H. Experimental study on shear performance of an advanced bolted connection in steel-concrete composite beams. *Case Stud. Constr. Mater.* **2022**, *16*, e01037. [\[CrossRef\]](#)
21. He, Z.-Q.; Ou, C.; Tian, F.; Liu, Z. Experimental Behavior of Steel-Concrete Composite Girders with UHPC-Grout Strip Shear Connection. *Buildings* **2021**, *11*, 182. [\[CrossRef\]](#)

22. Guo, J.; Zhou, Z.; Zou, Y.; Zhang, Z.; Jiang, J. Finite Element Analysis of Precast Concrete Deck-Steel Beam-Connection Concrete (PCSC) Connectors Using Ultra-High-Performance Concrete (UHPC) for the Composite Beam. *Buildings* **2022**, *12*, 1402. [[CrossRef](#)]
23. Jiang, H.; Sun, J.; Qiu, H.; Cao, D.; Ge, W.; Fang, Q.; Cui, H.; Chen, K. Cyclic Behavior of Multiple Hardening Precast Concrete Shear Walls. *Buildings* **2022**, *12*, 2069. [[CrossRef](#)]
24. Yaman, T.S.; Lucier, G. Shear Transfer Mechanism between CFRP Grid and EPS Rigid Foam Insulation of Precast Concrete Sandwich Panels. *Buildings* **2023**, *13*, 928. [[CrossRef](#)]
25. Liu, X.; Wang, X.; Yang, T.; Wu, Z. The Shear Behavior of Insulated Precast Concrete Sandwich Panels Reinforced with BFRP. *Buildings* **2022**, *12*, 1326. [[CrossRef](#)]

Disclaimer/Publisher's Note: The statements, opinions and data contained in all publications are solely those of the individual author(s) and contributor(s) and not of MDPI and/or the editor(s). MDPI and/or the editor(s) disclaim responsibility for any injury to people or property resulting from any ideas, methods, instructions or products referred to in the content.